Int. J. Heat Mass Transfer. Vol. 23, pp. 1045–1053
Pergamon Press Ltd. 1980. Printed in Great Britain

ANALYTICAL STUDY OF HEAT TRANSFER IN THE POST DRY-OUT REGION IN SMOOTH AND ROUGH VAPORIZATION CHANNELS

M. A. STYRIKOVICH, A. I. LEONTIEV, V. S. POLONSKY and I. I. MALASHKIN
Institute of High Temperatures of the U.S.S.R. Academy of Sciences, Moscow, U.S.S.R.

(*Received* 14 *January* 1977 *and in revised form* 27 *June* 1979)

Abstract — An analytical model is suggested for calculation of heat transfer in a post dry-out region which is based on the asymptotic turbulent boundary layer theory. High efficiency of artificial roughness in the enhancement of heat transfer under the conditions of a two-phase dispersed flow is shown. Treatment of a part of the experimental data obtained by the present authors and of some of the reported data in conformity with the suggested model of heat transfer in the post dry-out region has given a satisfactory agreement between the experiment and prediction.

NOMENCLATURE

D_d, diameter of drops [m];
T_{shv}, T_s, T_w, temperature of superheated vapour, saturated vapour and of the wall, respectively;
C_{fr0}, C_{fr}, friction coefficient of a smooth wall and friction coefficient under the conditions considered, respectively;
c_p, specific heat [kJ/kg K];
h_{01}, enthalpy of flow at the centre line of the channel up to convergence of thermal boundary layers [kJ/kg];
h_{vw}, h, h_{shv}, h', h'', enthalpy of vapour at the wall, of mixture, superheated vapour, water, and of satured vapour, respectively [kJ/kg];
Δh_v, specific latent heat of vaporization [kJ/kg];
Δh_Σ, $= h_{vw} - h_0$, differential in total enthalpies [kJ/kg];
m, volumetric concentration of drops [N/V^3];
n, power;
$\tilde{q}_0$, $= q_0/q_{w0}$, dimensionless heat flux under standard conditions [W/m^2];
$\tilde{q}$, $= q/q_w$, dimensionless heat flux under conditions considered [W/m^2];
v, v_{shv}, v', v'', specific volume of mixture, superheated vapour, water, and of saturated vapour, respectively [m^3/kg];
w_v, w_l, velocity of vapour and liquid, respectively [m/s];
$\tilde{w}_{0n}$, $= w_0/w_{01}$, relative axial velocity at the time of convergence of boundary layers;
x_b, balance void fraction;
x, x_0, flow quality at arbitrary location in the flow and at axial position in the channel, respectively;
z, space coordinate [m];
β, volumetric flow concentration;
δ_T, thermal boundary layer [m];
ξ, $= y/\delta_T$, dimensionless transverse coordinate;
ϑ, $= h/h_0$, dimensionless enthalpy;
λ, thermal conductivity of vapour [W/m K];
μ_0, characteristic axial viscosity [kg/m s];
ρ'', mass density of vapour [kg/m^3];
$\tilde{\rho}$, $= \rho/\rho_0$, relative flow density;
$\rho_0 w_0$, mass flow rate at the channel centre line [kg/m^2 s];
σ, surface tension [N/m];
Ψ_{sv}, Ψ_{sq}, Ψ_{sr}, relative limiting laws for heat transfer;
ψ, $= h_w/h_0$, enthalpy factor;
ω, $= w/w_0$, dimensionless velocity;
Nu, Nusselt number;
Pe, Peclet number;
Pr, Prandtl number;
Re_{D1}, Reynolds number in the dry-out cross-section;
Re_T^{**}, Reynolds number based on the energy loss thickness;
St, Stanton number for the conditions considered;
St_0, $= \dfrac{0.014}{Re_T^{**0.25} Pr_0^{0.75}}$, Stanton number for standard conditions;
We, Weber number.

1. INTRODUCTION

IN RECENT years much attention has been paid to the problems of heat transfer in dispersed two-phase flows motivated, apart from a pure scientific interest, by a variety of technological applications such as power engineering, metallurgy, aircraft and space technology, etc. The very first experiments have shown that in some cases the elements made of conventional materials can safely operate in a certain range of dispersed flow parameters. Further experiments were aimed at extension of the range of flow parameters, identification of the role of artificial roughness in the enhancement of heat transfer, and at the development of the mathematical model to describe the process.

In general, analytical studies were based on one-dimensional models. Of these, the investigations carried out by Miropolsky [1], Kalinin *et al.* [2], and Subbotin *et al.* [3] are best known in our country, while the relevant foreign efforts are represented by the works of Dougall [4], Forslung [5], and Laverty [6]. Moreover, there are a number of publications [7, 8] in which some of the ideas of the above authors are refined or developed further.

Analytical studies have provided a deeper insight into the peculiar features of heat and mass transfer downstream of the dry-out region, i.e. in the postcritical region, and made it possible to correlate the experimental data of different investigators as well as to obtain analytical relationships. However, a one-dimensional model does not allow the crosswise change of the flow parameters to be taken into account, which is indispensable for an adequate description of the process. As far as our knowledge goes, heat transfer in the postcritical region in rough vaporization channels has not yet been treated analytically.

2. PHYSICAL MODEL

Flow of a coolant in a steam generator is accompanied by changes in the flow structure. At high void fractions, a change in the boiling regimes in the postcritical region is associated with transition of the flow from a dispersed-annular pattern to a dispersed one. In the dispersed-annular flow the liquid phase is partially dispersed in the annular liquid film and partially in the flow itself in the form of drops (Fig. 1). In this flow region, heat transfer between the wall and the two-phase flow becomes greatly increased (portion AB). The wall temperature exceeds the temperature of saturation by only few degrees.

At the dry-out section of the channel a significant change in the heat-transfer conditions takes place. As the liquid film approaches this section it gets infinitesimally thin and then breaks. 'Dry' spots and islets of the incipient vapour film keep appearing and disappearing alternatively on the surface. Gradually, the boiling liquid film disappears and gives way to a continuous vapour film the thermal resistance of which is substantially higher. By convention, the cross-section in which the vapour boundary layer (averaged in time) is formed on a notable portion of the channel perimeter is usually taken for a burn-out heat-transfer cross-section. Starting with this cross-section, the wall temperature increases drastically (portion BC) and then, depending on the operating parameters, it may continue its growth or may decrease. At high mass flow rates and comparatively low void fractions, the heat-transfer coefficient attains its minimum, while the wall temperature reaches its maximum value, at the point C. At the point D, the wall temperature reaches its minimum value and then starts to increase again. At high void fractions and low mass flow rates the wall temperature, after a sharp increase, continues to rise but the rate of its change along the channel is much lower. On the portion AB the flow is slightly non-equilibrium due to metastable superheating (by several degrees) of the liquid adjacent to the wall. On the portion BC the flow becomes substantially non-equilibrium. Highly superheated vapour moves near the wall, while the drops of water occupy the core of the flow. As they come into the superheated vapour layer the drops evaporate, thereby increasing heat transfer between the wall and the flow. Some investigators indicate, however, that under these conditions the heat-transfer coefficient is still markedly lower than the predicted one for the flow of pure vapour. As will be shown below, this conclusion is due to disregard of the effect of non-isothermal conditions on the heat-transfer coefficient. Moreover, the heat transfer coefficient was calculated from the formulae for a stabilized flow.

The physical situation in the dry-out region rather bears a resemblance to the heat-transfer behaviour in the entry section of the channel. Starting from section 1-1 (Fig. 1), a thermal boundary layer develops the formation of which actually obeys the same laws which

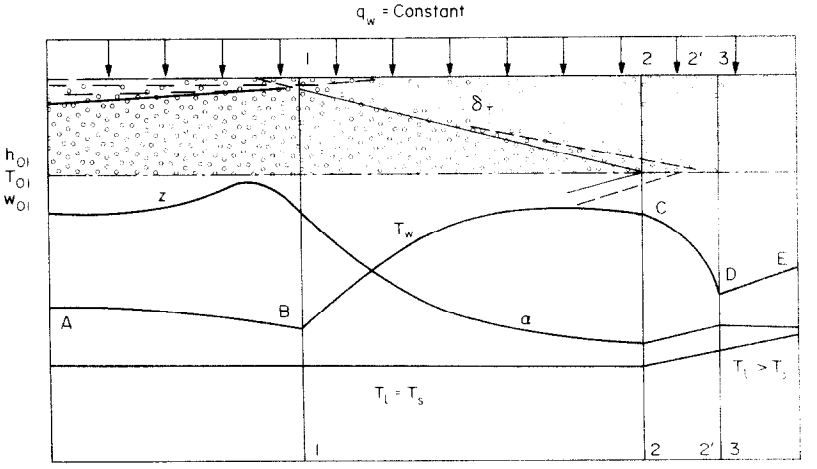

FIG. 1. Physical model of the process.

dominate in the inlet section of the channel. The dry-out cross-section may by convection be regarded as the front edge of the channel where the flow temperature is practically constant over the channel cross-section and equal to the saturation temperature. At high heat fluxes, when the wall temperatures in the postcritical region exceeds that of the maximum liquid superheat, $T_{\lim}$, the surface of the channel is washed by the superheated vapour, the temperature of which varies across the boundary layer from the wall temperature to the temperature of saturation in the flow core. By analogy with the thermal boundary layer one can analyse the diffusion boundary layer where the concentration of drops varies from the maximum in the flow core to zero at the wall or at some distance from it.

Drops of the liquid can evaporate only in a thermal layer δ_T and, therefore, it can be assumed that, up to the convergence of the thermal boundary layers, the enthalpy of the flow at the centre line of the channel will remain constant and equal to h_{01} in the dry-out section. The axial flow rate increases because of the growth of the boundary layer thickness and evaporation of drops. Increase in the boundary-layer thickness results in reduction of the heat-transfer coefficient and in the rise of the wall temperature up to section 2-2. On the portion BC increase in the flow rate due to evaporation of drops in the thermal boundary layer is insignificant because of a small size of this flow region. In section 2-2 the thermal boundary layers may be rather thick or they may even converge, so that the drops of liquid evaporate in a relatively large volume of the flow and thus with greater intensity. The vapour velocity on the portion CD of the channel increases rapidly which leads to an increase in the heat-transfer coefficient. However, vigourous evaporation of drops on the CD portion consumes a larger amount of heat supplied and thus decreases the rate of the flow temperature rise. Eventually, the flow rate proves to be the governing factor which determines the wall temperature on the portion CD. Therefore, in this portion the wall temperature decreases along the channel. Just after the point D the flow temperature increases and a rise in the wall temperature is observed. In the case of an intensive decrease in the heat flow rate due to evaporation of drops in a thermal boundary layer, the curve $T_w = T(\tilde{z})$ may show deflection even before the layers will converge in section 2'-2'.

The liquid drops are of a relatively small size. Usually, the critical Weber number is taken to be

$$We_{cr} = \frac{D_d \rho''(w_v - w_l)^2}{\sigma} = 7.5.$$

As soon as this value is reached, the drops start to break. Generally it is assumed that a drop splits into two approximately equal drops. Under the dry-out conditions the average size of drops is 10^{-5}–10^{-3} m. Despite such small dimensions the drops may persist up to very high balance void fractions, i.e. throughout a highly superheated vapour flow. It has been indicated in a number of experimental studies that drops remain present in the flow up to $x_b = 2$–3. It should be noted, however, that this phenomenon was observed with freon, for which the ratio r/c_p is much lower than for water. Accordingly, the vapour superheat at $x_b = 2$–3 is considerably lower than that for the steam–water mixture under similar conditions, which means that the rate of drop evaporation is comparatively low.

Since the size of drops is small, one can assume the flow to be homogeneous. The extent to which the real flow approaches a homogeneous one is the higher, the lower the volumetric fraction of the liquid phase $(1 - \beta)$. Since the evaporation rate of drops is small, their concentration throughout the flow will be mainly determined by turbulent diffusion. In this respect, heat transfer between evaporating drops and the vapour flow is similar to the process of heat transfer in dissociating or chemically reacting gases in a 'frozen' boundary layer at the inlet into the channel under the conditions of substantially varying flow density.

Evaporation of drops is most vigorous close to the wall. In the first approximation it can be assumed that the drops evaporate in a thin layer adjacent to the wall and that distribution of their concentration across the boundary layer is determined by turbulent diffusion and is similar to the distribution of velocities and enthalpies of the mixture. Such a model resembles a 'frozen' flow of gas which reacts chemically with the surface of the channel. Chemical reactions take place in a thin flame front, while distribution of the concentration of species over the boundary cross-section is determined by turbulent diffusion. The flame front can be located both at the wall (heterogeneous burning) and at some distance from it (homogeneous burning). An analogue of the flame front under the discussed conditions is the region of intensive and complete evaporation of drops. In conformity with the model adopted, the rate of convective heat transfer between the tube and the moist vapour will be greatly affected by variation of the mixture density across the boundary layer as well as by heat loss in the region of vigorous evaporation of drops. These effects can be taken into account by the use of the asymptotic boundary-layer theory presented elsewhere [9].

3. TREATMENT OF EXPERIMENTAL DATA. A SET OF EQUATIONS

In general, the relative limiting law for heat transfer can be written as

$$\Psi_s = \left(\frac{St}{St_0}\right)_{Re_T^{**}} = \left[\int_0^1 \left(\tilde{\rho}\frac{\tilde{q}_0}{\tilde{q}}\frac{\partial\omega}{\partial\xi}\frac{\partial\vartheta}{\partial\xi}\right)^{1/2} \mathrm{d}\xi_T\right]^2. \tag{3.1}$$

Let us consider a diffusion non-equilibrium vapour-drop flow model taking into account the assumptions adopted. Write down the following system of equations:

$$\begin{cases} \dfrac{h_w - h}{h_w - h_0} = \dfrac{1 - x}{1 - x_0} = \omega, & (3.2) \\ v = v_v x + v'(1 - x), & (3.3) \\ v_v = v'' + \dfrac{\partial v}{\partial h}(h_v - h), & (3.4) \\ h = h_v x + h'(1 - x). & (3.5) \end{cases}$$

It has been shown in [9] that a combined effect of different perturbation factors on the heat-transfer law for a turbulent boundary layer can be represented as the product of relative heat-transfer laws allowing for separate effect of each of these factors. Since

$$\frac{\partial \omega}{\partial \xi_T} = \frac{\partial \vartheta}{\partial \xi_T} \quad \text{for } \tilde{q}_0/\tilde{q} \simeq 1 \text{ (no internal heat sinks)},$$

the limiting law of heat transfer can be given as

$$\Psi_{sv} = \left[\int_0^1 \frac{\mathrm{d}\omega}{\sqrt{\tilde{v}}}\right]^2. \quad (3.6)$$

Solution of the system of equations (3.2)–(3.5) yields

$$\tilde{v} = \frac{v_w}{v_0} - \left(\frac{v_w}{v_0} - 1\right)\omega. \quad (3.7)$$

The limiting heat-transfer law can be finally written as

$$\Psi_{sv} = \left(\frac{2}{\sqrt{(v_w/v_0) + 1}}\right)^2. \quad (3.8)$$

As will be shown below, by using the parameter Ψ_{sv} one can satisfactorily correlate the experimental data on heat transfer in the dry-out zone. The effect of decrease in the internal heat flow rate (evaporation of drops in the superheated vapour boundary layer) on the heat-transfer law is determined for a mixture flow with constant density $\tilde{\rho} = 1$. Then the limiting relative heat transfer law can be given as

$$\Psi_{sq} = \left[\int_0^1 (\tilde{q}_0/\tilde{q})^{1/2}\,\mathrm{d}\vartheta\right]^2. \quad (3.9)$$

Making use of the approximation $\tilde{q}/q_0$ suggested in [9], we obtain

$$\tilde{q}_0/q = 1 + \frac{St^{-1}\int_0^{\xi_T} \tilde{q}_v \mathrm{d}\xi_T}{1 + 2\xi_T}, \quad (3.10)$$

where

$$\tilde{q}_v = \frac{q_v \delta_T}{\rho_0 w_0 \Delta h_\Sigma}.$$

A decrease in the volumetric heat rate due to drop evaporation q_v can be written as

$$q_v = 2\pi D_d m(T_v - T_s)\lambda_v. \quad (3.11)$$

It is assumed in the expression for q_v that the Nusselt number, Nu, has a value of two. Concentration of drops can be obtained from the following expression:

$$\frac{m\pi D_d^3 \gamma'}{6\gamma_{\mathrm{mix}}} = 1 - x. \quad (3.12)$$

Since

$$\gamma_{\mathrm{mix}} = \frac{1}{v_{\mathrm{mix}}} = \frac{1}{v_w - \omega(v_w - v_0)}, \quad (3.13)$$

and assuming $\omega = \xi_T^n$, we obtain

$$1 - x = (1 - x_0)\xi_T^n, \quad (3.14)$$

$$m = \frac{6(1 - x)\xi_T^n}{\pi D_d^3 \gamma'[v_w - \xi_T^n(v_w - v_0)]}. \quad (3.15)$$

The system of equations (3.2)–(3.5) yields

$$T_v - T_s = (T_w - T_s)(1 - \xi_T^n).$$

Thus,

$$q_v = \frac{12\lambda_v(1 - x_0)(T_w - T_s)(1 - \xi_T^n)\xi_T^n}{D_d^2 \gamma'[v_w - \xi_T^n(v_w - v_0)]}. \quad (3.16)$$

Since the effect of $\tilde{q}_0/\tilde{q}$ on the heat-transfer law is relatively small, we shall simplify the expression for q_v by omitting the term $\xi_T^n(v_w - v_0)$ in the denominator and taking for the wall temperature its value in the extreme cross-section, $T_w^{\max}$.

Finally, we get

$$q_v = A(1 - \xi_T^n)\xi_T^n, \quad (3.17.1)$$

where

$$A = \frac{12\lambda_v(1 - x_0)(T_w^{\max} - T_s)}{D_d^2 \gamma' v_w}. \quad (3.17.2)$$

The numerator in equation (3.10) can be written as

$$St^{-1}\int_0^{\xi_T} \tilde{q}_v \mathrm{d}\xi_T = \frac{A\delta_T}{q_w}\left(\frac{\xi_T^{n+1}}{n+1} - \frac{\xi_T^{2n+1}}{2n+1}\right). \quad (3.18)$$

By approximating

$$\frac{\xi_T^{n+1}}{1 + 2\xi_T} = 0.41\,\xi_T \quad \text{and} \quad \frac{\xi_T^{2n+1}}{1 + 2\xi_T} = 0.375\,\xi_T$$

we obtain

$$\frac{\tilde{q}_0}{\tilde{q}} = 1 + \frac{A\delta_T}{q_w}\left(\frac{0.41\,\xi_T}{n+1} - \frac{0.375\,\xi_T}{2n+1}\right), \quad (3.19)$$

while the expression for Ψ_{sq} takes on the form

$$\Psi_{sq} = \left[\int_0^1 \sqrt{(1 + a\xi_T)}\,\mathrm{d}\vartheta\right]^2 \quad (3.20.1)$$

where

$$a = \frac{0.067\,A\delta_T}{q_w}. \quad (3.20.2)$$

Replacing ξ_T by $\vartheta - \xi_T = \vartheta^{1/n}$, assuming $n = 1/7$, and approximating the expression for ϑ^7 by $0.25\,\vartheta$, we finally get

$$\Psi_{sq} = \left\{\frac{8}{3a}\left[\left(1 + \frac{a}{4}\right)^{3/2} - 1\right]\right\}^2. \quad (3.21)$$

The effect of the heating surface roughness on heat transfer can be taken into account in the following way. It is shown in [10, 11] that the St number increases directly with a 'pure' friction coefficient, the

latter being a part of the total coefficient of resistance, i.e.

$$\Psi_{sr} = (C_f^{fr}/C_{f0}^{fr})_{Re}, \tag{3.22}$$

where C_f^{fr} is the friction coefficient under the conditions considered (without regard for the resistance of roughness), and C_{f0}^{fr} is the friction coefficient of a smooth wall. The problem is thus reduced to extraction of the 'pure' friction coefficient from the total coefficient of resistance, the technique of which is discussed in a number of publications. Thus, according to [12], it can be assumed that

$$C_f^{fr} = \frac{C_f}{(Re/5000)^{0.25}}, \tag{3.23}$$

while according to [13]

$$C_f^{fr} = C_{f0}^{fr}\sqrt{(C_f/C_{f0}^{fr})}. \tag{3.24}$$

Based on the above, the predicted value of St can be determined as

$$St_{pr} = St_0\Psi_{sv}\Psi_{sq}\Psi_{sr}. \tag{3.25}$$

Under standard conditions, the heat-transfer law in the inlet section is described by

$$St_0 = \frac{B}{2Re_T^{**0.25}Pr_0^{0.75}} = \frac{0.014}{Re_T^{**0.25}Pr_0^{0.75}}. \tag{3.26}$$

The experimental value of St can be found from

$$St_{ex} = \frac{q_w D}{(Re_{D1} + 5.2\psi Re_T^{**})\mu_0\Delta h}. \tag{3.27}$$

The number Re_T^{**} can be found from the energy equation

$$\frac{dRe_T^{**}}{d\tilde{z}} + \frac{Re_T^{**}}{\Delta h}\frac{d\Delta h}{d\tilde{z}} + \frac{Re_T^{**}}{\rho_0 u_0}\left(\frac{\delta_T}{\delta_T^{**}}\right)\frac{D}{\Delta h}\int_0^1 \tilde{q}_v d\xi_T = St\,Re_D. \tag{3.28}$$

The distribution $\Delta h = h(\tilde{z})$ is known from experiment.

Assuming that

$$\left(\frac{\delta_T}{\delta_T^{**}}\right)\frac{D}{\rho_0 u_0 \Delta h}\int_0^1 \tilde{q}_v d\xi_T = c = \text{constant} \tag{3.29}$$

yields a linear inhomogeneous equation, it can be solved as follows:

$$Re_T^{**} = \frac{q_w D}{\mu\Delta h}\left[\frac{e^{cz} - 1}{c\,e^{cz}}\right]. \tag{3.30}$$

The value of c is of the order of hundredths or thousandths. For small values of c ($c \to 0$), the latter equation can be approximated by

$$Re_T^{**} = \frac{q_w D}{\mu_0 \Delta h}\cdot\frac{\tilde{z}}{1 + c\tilde{z}}.$$

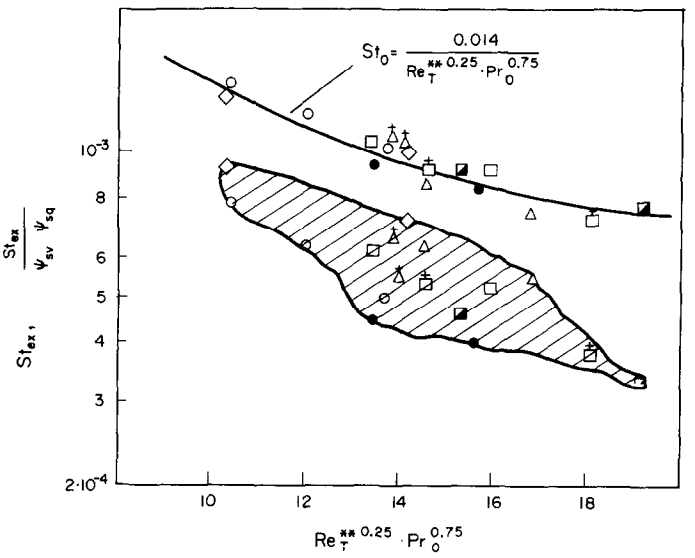

□ - P = 98	q = 750	ρw = 1400	x_B = 0.5	(R1)
◪ - P = 13.7	q = 656	ρw = 950	x_B = 0.38	(R17)
○ - P = 13.7	q = 580	ρw = 1000	x_B = 0.38	(R17)
● - P = 14.7	q = 214	ρw = 682	x_B = 0.38	(R17)
△ - P = 16.7	q = 160	ρw = 580	x_B = 0.61	(R16)
◇ - P = 9.8	q = 682	ρw = 1000	x_B = 0.75	
○ - P = 9.8	q = 750	ρw = 1000	x_B = 0.78	
○ - P = 13.7	q = 750	ρw = 1250	x_B = 0.51	
○ - P = 13.7	q = 750	ρw = 1000	x_B = 0,63	(a)
○ - P = 13.7	q = 721	ρw = 1000	x_B = 0.47	
⛛ - P = 16.7	q = 450	ρw = 700	x_B = 0.39	
⛝ - P = 16.7	q = 700	ρw = 1250	x_B = 0.45	

FIG. 2. Dependence of St_{ex} and $St_{ex}/\Psi_{sv}\Psi_{sq}$ on $Re_T^{**0.25}Pr_0^{0.75}$. (a) Data of the present work.

The parameters h_0, v_0, μ_0, u_0 and others on the flow axis are determined from ordinary equations for two-phase flows. The wall parameters are determined from pressure P and temperature T_w. The slip ratio in the equation for the drop diameter can be estimated by conventional techniques, for example, as those described in [14].

4. DISCUSSION OF EXPERIMENTAL DATA

The experimental data of the present authors as well as those reported in [15–17] have been treated in accordance with the model suggested. The results of this analysis are presented in Figs. 2–5. The predicted values of St are given in the dashed region of Fig. 2 as a function of the parameter $Re_T^{**0.25} \cdot Pr_0^{0.75}$. As seen from this fig., in some cases deviation from the curve $St_0 = 0.014/Re_T^{**0.25}\ Pr_0^{0.75}$ is about 200–300%. The use of the parameters Ψ_{sv} and Ψ_{sq} bring these data closer to the theoretical curve.

It should be noted that the experimental data obtained at small volumetric water contents in the flow, fall close to the theoretical curve. With increase in water content, the experimental values of $St_{ex}/\Psi_{sv}\Psi_{sq}$ start to deviate from the theoretical values. The same is observed for the data obtained in the case when the wall temperature in postcritical conditions over the inlet section of the channel is less than the limiting temperature of the liquid superheat $T_{\lim}$ ($T_{\lim}$ is taken from [18]). This signifies the development of a two-phase boundary layer with unknown vapour content. The value of h_w calculated from the wall temperature and pressure is noticeably higher than the actual one. This will naturally lead to a significantly underestimated value of $St_{ex}/\Psi_{sv}\Psi_{sq}$ as compared with St_0.

Figure 3 presents the treated experimental data for a rough surface in the coordinates $St_{ex}/\Psi_{sv}\Psi_{sq}$ vs. $Re_T^{**0.25}\ Pr_0^{0.75}$. As is seen from the fig., the heat-transfer rate at the rough surface is considerably higher than at a commercially smooth one.

In order to calculate Ψ_{sr}, calibration has been made of the hydraulic resistances for commercially smooth and rough portions of the channel. The results are shown in Fig. 4. The coefficient of hydraulic resistance C for the smooth portion in the studied range of the Re_D numbers is 0.0235. The hydraulic resistance coefficient C_f for a rough surface varied from about 0.042 at $Re_D = 7 \times 10^4$ to about 0.046 at $Re_D = 4.5 \times 10^5$.

The value of C_f^{fr}/C_{f0} was calculated using the method suggested by Gomelauri [13]. The results for the rough surface, with Ψ_{sr} taken into account, approach the theoretical curve. The observed deviation from the predicted points does not exceed 30–35%. It should be noted, however, that for the most part the experimental points lie above the theoretical curve. When Ψ_{sr} is calculated from a somewhat different formula than that proposed by Gomelauri, namely from $\Psi_{sr} = (C_f/C_{f0})^{0.7}$, then the calculated data fall close to the theoretical curve.

5. PREDICTION OF HEAT TRANSFER IN THE POSTCRITICAL REGION

The analysis of the experimental data has shown that the heat transfer law for the initial section of the postcritical region can be described by equation (3.25). The relation $St = f(Re_T^{**}, \ldots)$ combined with the energy and discontinuity equations, makes it possible to calculate heat transfer from the length of the inlet section. In the first approximation the energy equation is used without the term which takes into account the decrease in the heat flow rate due to evaporation of drops. Their influence on the St number is taken into consideration in the heat transfer law Ψ_{sq}. The energy equation has two unknowns, namely Re_T^{**} and Δh. For

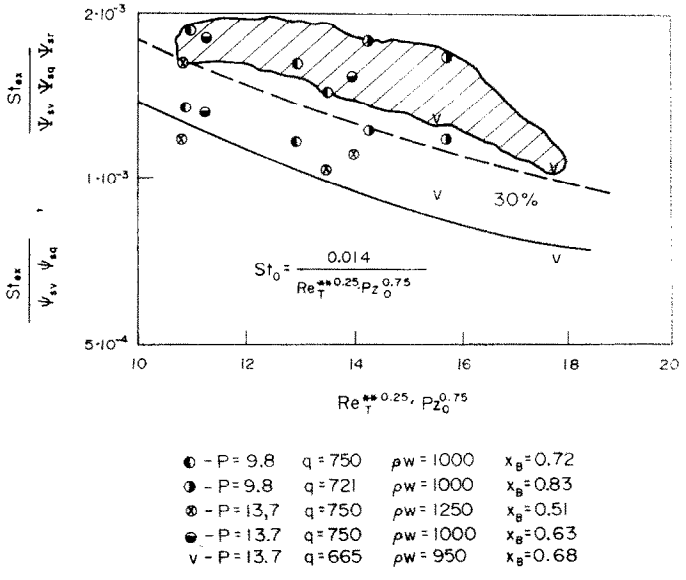

FIG. 3. Dependence of $St_{ex}/\Psi_{sv}\Psi_{sq}$ and $St_{ex}/\Psi_{sv}\Psi_{sq}\Psi_{sr}$ on $Re_T^{**0.25}\ Pr_0^{0.75}$.

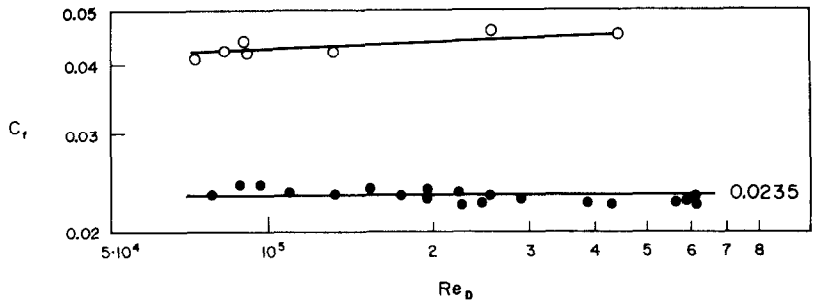

FIG. 4. Relationship $C_f = C(Re_D)$.

these to be determined, we shall make use of the above relation. Since Ψ_{sv} depends on h_w, the relation should be supplemented with an additional condition which would permit the flow density to be given in terms of the enthalpy. The expression for Ψ_{sv} is approximated as follows:

$$\Psi_{sv} = \left(\frac{2}{\sqrt{(v_w/v_0)+1}}\right)^2 = \frac{2.2}{1+v_w/v_0}. \quad (5.1)$$

This equation describes the relative heat transfer law in the range $2 \le v_w/v_0 \le 6$ rather adequately.

The specific volume of the mixture on the channel axis in the inlet section can be expressed in terms of the enthalpy at the entrance plane,

$$v_0 = l + dh_0, \quad (5.2)$$

where

$$l = v' - (v'' - v')h'/r, \quad d = \frac{v'' - v'}{r}.$$

The specific vapour volume on the wall, as mentioned above, is

$$v_w = v'' + \partial v/\partial h(h_w - h''), \quad (5.3)$$

in which

$$\partial v/\partial h = \frac{\Delta v_{sh}}{\Delta h_{sh}} = \frac{v_{sh} - v''}{h_{sh} - h''}.$$

Then

$$\Psi_{sv} = \frac{2.2}{c_1 + d_1\psi} \quad (5.4)$$

where

$$c_1 = \frac{v'' - h''(\partial v/\partial h)}{l + dh_0} + 1, \quad d_1 = \frac{h_0(\partial v/\partial h)}{l + dh_0},$$

and equation (3.25) takes on the form

$$St = \frac{B\Psi_{sr}}{Re_T^{**0.25} Pr_0^{0.75}(c_1 + d_1\psi)}. \quad (5.5)$$

At q_w = constant, the integral of the energy equation (without q_v) is

$$Pe^{**} = \frac{N\tilde{z}}{\psi - 1}, \quad (5.6.1)$$

or

$$\psi = 1 + \frac{N\tilde{z}}{Pe^{**}}, \quad (5.6.2)$$

in which

$$Pe^{**} = Re_T^{**} Pr_0, \quad Nu = \frac{q_w D c_p}{h_0 \lambda}.$$

Assuming that

$$St = \frac{N}{Pe_D(\psi - 1)} = \frac{1.1\, B\Psi_{sr}}{Pe^{**0.25} Pr_0^{0.5}(c_1 + d_1\Psi)} \quad (5.7)$$

and

$$Pe_D = Pe_{D1} + 5.2\,\psi Pe^{**}, \quad (5.8)$$

(a detailed derivation of these equations is given in [9]), we obtain a system of three equations (5.6–5.8) with three unknown quantities ψ, Pe^{**} and Pe_D. By solving the system with respect to $\tilde{z}$, we obtain

$$\tilde{z} = 3.36\, N^{-1}\left[\frac{d_1 N Pr_0^{0.5} Pe^{**0.25}}{\Psi_{sr}} - 0.0286\, Pe_{D1} - 0.149\, Pe^{**} + \sqrt{\left[\left(\frac{d_1 N Pr_0^{0.5} Pe^{**0.25}}{\Psi_{sr}} - 0.0286\, Pe_{D1} - 0.149\, Pe^{**}\right)^2 + \frac{0.595(c_1 + d_1) Pr_0^{0.5} Pe^{**1.25} N}{\Psi_{sr}}\right]}\right]. \quad (5.9)$$

From a knowledge of Pe^{**} we determine $\tilde{z}$, and from equation (5.6.2) we find ψ. The length of the inlet section can be determined based on the following arguments. When the boundary layers converge the relative axial velocity [9] is

$$\tilde{w}_{0n} = \frac{w_0}{w_{01}} = \left(1 - 2.6\frac{\delta^{**}}{Re_0}\psi\right). \quad (5.10)$$

Taking into account that

$$\frac{\delta^{**}}{Re_0} = 0.074\,\psi^{-0.318} \quad (5.11)$$

and

$$\tilde{w}_{0n} = \frac{Pe_D}{Pe_{D1}}, \tag{5.12}$$

we get

$$Pe_{D1} + 5.2\psi Pe^{**} = \frac{Pe_{D1}}{1 - 0.192\psi^{0.682}}. \tag{5.13}$$

Thus, for determination of the length of the inlet section $\tilde{z}_{in}$, we have a system of three equations (5.6), (5.9), and (5.13). This system cannot be solved with respect to the variables $\tilde{z}_{in}$, Pe^{**}, and ψ. The value of $\tilde{z}_{in}$ is found from a grapho-analytical estimation of the system. In particular, by ascribing the values of Pe^{**} from equation (5.9), we determine $\tilde{z}$. From equation (5.6.2) we obtain the value of ψ and plot the relation

$$\psi = f\left(\frac{\tilde{z}}{Pe^{**}}\right).$$

By solving equation (5.13) with respect to Pe^{**} we get

$$Pe^{**} = \frac{Pe_{D1}\psi^{0.682}}{5.2\psi(5.21 - \psi^{0.682})}.$$

Then, from equation (5.14) we find $Pe^{**} = f_1(\psi)$. The point of intersection of $\psi = f(\tilde{z}/Pe^{**})$ with $Pe^{**} = f_1(\psi)$ yields the values of ψ_{in} and Pe^{**}_{in}, and hence from equation (5.9) we obtain the value of $\tilde{z}_{in}$. The length of the inlet section can also be determined from the departure of the calculated points from the curve for the heat transfer law.

Figure 5 compares the experimental and predicted points in the traditional coordinates $T_w = T(l/d)$. The data were calculated in accordance with recommendations given in Sections 3 and 5. Figure 5 shows a satisfactory agreement between the predicted and experimental results. It should also be noted that the predicted values for the length of the inlet section $\tilde{z}_{in}$ somewhat exceed the experimental ones. This points to the fact that in estimating $\tilde{z}_{in}$ no account was taken of the parameter Ψ_{sq} which is responsible for the deflection of the curve $T_w = T(l/d)$.

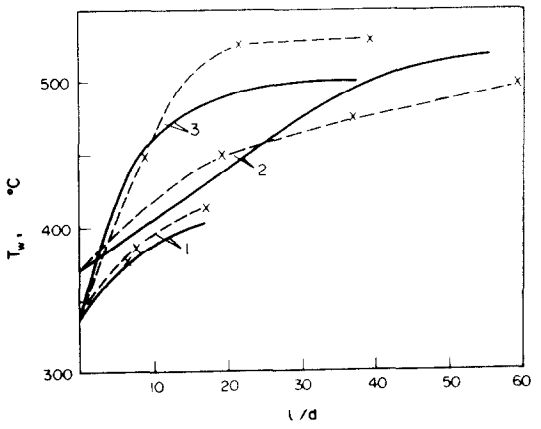

FIG. 5. Dependence of the predicted and experimental wall temperatures on the relative length of the channel: (a) prediction, (b) experiment. (1) $P = 98$ bar, rough section; (2) $P = 167$ bar, smooth section; (3) $P = 98$ bar, smooth section.

The suggested model has been verified and can be recommended for the use in the following range of parameters: $P = 98$–167 bar; $\rho w = 500$–$1400\,\text{kg/m}^2\,\text{s}$; $x \geq 0.38$; $q_w \geq 214\,\text{kW/m}^2$, and $a < 1.0$. It should be noted, however, that the verification has been made only on the basis of the final value of T_w. Therefore, a satisfactory agreement between the predicted and experimental values of the wall temperature is insufficient to check the physical validity of the model. For a more rigorous checking of this model it is desirable to carry out a number of experiments involving measurement of intermediate values along the channel length (e.g. mean flow rate vapour temperature or mean flow rate vapour quality). Extension of the proposed method to other ranges of parameters requires an additional verification.

REFERENCES

1. Z. L. Miropolsky, Heat transfer in film boiling of vapour water mixture in vaporization tubes, *Teploénergetika* **5**, 49–52 (1963).
2. E. K. Kalinin, I. I. Berlin, V. V. Kostyuk and Yu. S. Kochelaev, *General and Theoretical Problems of Thermo- and Helioenergetics*, Vol. 3. VINITI, Moscow (1972).
3. V. I. Subbotin, O. V. Remizov and V. A. Vorobiyov, Temperature regimes and heat transfer in the region of reduced heat exchange, *Teplofiz. Vysok. Temper.* **11**, 1220–1226 (1973).
4. R. S. Dougall and W. M. Roshenow, Film boiling on the inside of vertical tubes with upward flow of the fluid at low qualities, Dept. Mech. Engng, Mass. Inst. Technol. Rept. No. 9079, 29 (1963).
5. R. P. Forslung and W. M. Rohsenow, Thermal non-equilibrium in dispersed flow film boiling in a vertical tube, Dept. Mech. Engng, Mass. Inst. Technol. Rept. No. 75312, 44 (1966).
6. W. F. Laverty and W. M. Rohsenow, Film boiling of saturated nitrogen flowing in the vertical tube, *J. Heat. Transfer* **89(C)**(1), 90–98 (1967).
7. A. A. Bishop, R. P. Sandbery and L. S. Tong, Forced convection heat transfer to water after the critical heat flux at high subcritical pressure, CAP-2056, pt. V. Westinghouse Electric Corp., Pittsburgh (1965).
8. M. Cumo, *Elementi di Termotecnika de Reattora*. Camitato Nazionale Energia Nucleare, Roma (1971).
9. S. S. Kutateladze and A. I. Leontiev, *Heat and Mass Transfer in a Turbulent Boundary Layer*. Energiya, Moscow (1972).
10. A. A. Gukhman, *Application of Similarity Theory to the Study of Heat and Mass Transfer Processes*. Vyssh. Shkola, Moscow (1967).
11. E. K. Kalinin, G. A. Dreitser and S. A. Yarkho, *Intensification of Heat Transfer in Channels*. Mashinostroyeniye, Moscow (1972).
12. V. K. Migai, Heat transfer in rough tubes, *Izv. Akad. Nauk SSSR, Energ. Transp.* **3**, 97–107 (1968).
13. V. I. Gomelauri, R. D. Kandelaki and M. E. Kipshidze, Intensification of convective heat transfer under the action of artificial roughness, in *Problems of Convective Heat Transfer and Purity of Water Vapour*, pp. 137–140. Metsnierebe, Tbilisi (1970).
14. Z. L. Miropolsky, Flow quality of the forced circulation vapour–water mixture with addition of heat and under adiabatic conditions, *Teploénergetika* No. 5, 60–63 (1971).
15. V. E. Doroshchuk, *Crisis of Heat Transfer in Water Boiling in Tubes*. Energiya, Moscow (1970).
16. A. S. Konkov, Experimental study of the conditions of

heat transfer reduction for the vapour–water mixture flow in heated tubes, *Trudy TsKTI* **58**, 170–178 (1965).
17. M. A. Styrikovich and V. S. Polonsky, Experimental study of the effect of artificial roughness on post dry-out heat transfer, *5th Int. Heat Transfer Conference*, B41, 145–149, Tokyo (1974).
18. V. P. Skripov, *Metastable Liquid*. Science, Moscow (1972).

ETUDE ANALYTIQUE DU TRANSFERT THERMIQUE DANS LA REGION DE POST-ASSECHEMENT DANS DES CANAUX LISSES OU RUGUEUX DE VAPORISATION

Résumé — On propose un modèle analytique pour le calcul du transfert thermique dans la région de post-assèchement, basé sur la théorie asymptotique de la couche limite turbulente. On montre la haute efficacité de la rugosité artificielle dans l'accroissement du transfert sous les conditions d'un écoulement dispersé diphasique. Une partie des données expérimentales obtenues par les auteurs et d'autres données en conformité avec le présent modèle sont traitées en montrent un accord satisfaisant entre l'expérience et la prévision.

BERECHNUNG DES WÄRMEÜBERGANGS NACH DEM "DRY-OUT" IN GLATTEN UND RAUHEN ROHREN

Zusammenfassung—Zur Berechnung des Wärmeübergangs nach dem "dry-out" wird ein Rechenmodell auf der Grundlage der Theorie der turbulenten Grenzschicht vorgeschlagen. Die große Wirksamkeit künstlicher Rauhigkeiten bei der Verbesserung des Wärmeübergangs disperser Zweiphasenströmung wird gezeigt. Für den Bereich nach dem dry-out ist die Übereinstimmung zwischen einem Teil der Versuchsergebnisse der Autoren und den aus dem Modell berechneten Werten zufriedenstellend.

АНАЛИТИЧЕСКОЕ ИССЛЕДОВАНИЕ ТЕПЛООБМЕНА В ЗАКРИЗИСНОЙ ОБЛАСТИ ГЛАДКИХ И ШЕРОХОВАТЫХ ПАРОГЕНЕРИРУЮЩИХ КАНАЛОВ

Аннотация — Предложена аналитическая модель расчёта теплообмена в закризисной области, основанная на асимптотической теории турбулентного пограничного слоя. Показана высокая эффективность искусственной шероховатости в интенсификации теплообмена в дисперсном режиме течения двухфазного потока. Обработка части опытов авторов и ряда опытов других исследователей в соответствии с предложенной моделью процесса теплообмена в закризисной области показала удовлетворительную сходимость экспериментальных и расчетных данных.